ELSEVIER

Applied Catalysis B: Environmental 19 (1998) 45–57

APPLIED CATALYSIS B: ENVIRONMENTAL

Kinetics and mechanism of the reduction of nitric oxides by H_2 under lean-burn conditions on a Pt–Mo–Co/α-Al_2O_3 catalyst

Brigitta Frank[1], Gerhard Emig[2], Albert Renken[*]

Laboratory of Chemical Reaction and Electrochemical Engineering (LGRC), Swiss Federal Institute of Technology (EPFL), CH - 1015 Lausanne, Switzerland

Received 1 March 1998; received in revised form 6 April 1998; accepted 28 May 1998

Abstract

The kinetics and the mechanism of the selective reduction of nitric oxides (NO_x) by hydrogen is studied on a trimetallic Pt–Mo–Co/α-Al_2O_3 catalyst under oxidising conditions. This system is interesting in view of an exhaust gas control of power plants or lean-burn cars. It can be shown that the NO dissociation is the crucial step, dominating the overall reaction behaviour and that it depends on temperature and on the partial pressure of H_2. With increasing temperatures the reaction reveals an autocatalytic behaviour resulting in bistability and hysteresis. At higher temperatures, where no bistability is found, the NO/H_2 as well as the competing O_2/H_2 reaction occur only above a certain critical partial pressure of H_2. The kinetics of the NO/H_2/O_2 reaction are established using a modified Langmuir–Hinshelwood model (T=142°C–160°C, y_{O_2}>4%) which takes into account the critical H_2 partial pressure. The model describes the experimental data within ±15%. The determined activation energies are: 63 kJ/mol for the NO_x consumption, 77 and 45 kJ/mol for the N_2 and N_2O formation, respectively, and 130 kJ/mol for the O_2/H_2 reaction. Adsorption enthalpies are determined to −59 kJ/mol for the adsorption of H_2, −77 kJ/mol for the adsorption of NO and −97 kJ/mol for the adsorption of O_2. An interesting feature of the reaction is the enhancement of the NO/H_2 reaction by oxygen for low partial pressures of O_2. This appears to be the first study where a promoting effect of oxygen for the NO/H_2 reaction is found on a platinum supported catalyst.

Keywords: NO_x; Hydrogen; Lean-burn; Exhaust gas; Kinetics; Mechanism; Pt–Mo–Co supported catalyst

1. Introduction

Today, the concern about carbon dioxide emissions leads to the demand of lean-burn petrol engines and improved diesel engines. Both engines work under oxidising conditions where an appreciable lower quantity of fuel is needed and consequently less carbon dioxide is produced. For the moment this development is mainly restricted to Europe and Japan, where fuel is expensive compared to the United States. The main problem in oxidising atmospheres is the reduction of NO, since the actually used three-way catalyst in automobiles using Pt, Pd and Rh is not able to reduce nitric oxide under oxidising conditions.

Since relatively few knowledge existed up to the 1990's to reduce NO_x, CO and hydrocarbon emissions

*Corresponding author. Tel.: +41-21-693-3181; fax: +41-21-693-3690; e-mail: albert.renken@epfl.ch

[1]LONZA AG, Walliser Werke, CH - 3930 Visp, Switzerland.

[2]Lehrstuhl für Technische Chemie I, Universität Erlangen-Nürnberg, D - 91058 Erlangen, Germany.

0926-3373/98/$ – see front matter
PII: S0926-3373(98)00057-5

in an overall oxidising atmosphere, much activity has been done in this subject since then. Up to now the reduction of NO under oxidising conditions using platinum catalysts was mostly investigated using hydrocarbons [1–5]. Hydrogen as reducing agent, which is also present in the exhaust of automobiles, is only considered in few studies [6,7]. Wildermann [8] showed that the reduction of nitric oxide by hydrogen can be achieved under oxidising conditions (8% O_2) as present in the exhaust gas of power plants. A Pt–Mo catalyst supported on α-Al_2O_3 appeared to be the most effective one when water is present in the exhaust gas [8]. Hydrogen might be used to reduce NO_x emissions of stationary sources or of automobiles. It was further shown that Co as third component increases the NO reduction activity of the Pt–Mo/α-Al_2O_3 catalyst in an oxidising atmosphere when up to 0.6% CO are present [9]. This CO concentration corresponds to that present in the exhaust of lean-burn cars. Trimetallic catalysts are often found to be superior to bi- or monometallic catalysts. Another group reported recently that the addition of Na and Mo to a Pt/SiO_2 catalyst improves the reaction characteristics of the NO_x reduction by CO and hydrocarbons under lean static conditions [10].

These features suggest that the Pt–Mo–Co catalyst is an interesting candidate for an application in exhaust-gas control under lean-burn conditions. Such a catalyst is further desirable since it does not contain the scarce and thus expensive metal Rhodium.

In the present study the reduction of NO_x by H_2 is, therefore, examined on the 0.2% Pt–0.7% Mo–0.1% Co/α-Al_2O_3 catalyst under oxidising conditions (5–11% O_2). Furthermore a modelling of the $NO/H_2/O_2$ reaction is undertaken and kinetic data are estimated. Nowadays, simulations are effected in an increasing number of studies [11,12] in order to optimise the efficiency of a catalyst. To simulate the complex behaviour of exhaust gas reactions under lean-burn conditions kinetic data are needed. However, only few kinetic data for the reduction of NO in oxidising atmospheres exist.

2. Experimental

The experimental set-up used in this work is shown in Fig. 1 and consists of three parts: gas supply, recycle loop reactor and analysis part. As gases CO and NO and H_2 (all 10% in Ar), O_2 and Ar are used with purities of >99.996% (NO 99.9%) without further treatment (Carbagas, CH). Gases are supplied by mass flow controllers (F-201, Bronkhorst, NL).

In all experiments 0.75 g of a 0.2% Pt–0.7% Mo–0.1% Co catalyst supported on α-Al_2O_3 is used (particle diameter $1<d_p<1.25$ mm) which is prepared by a dry impregnation technique [8]. The BET-surface of the catalyst is below 3 m^2/g and the mean pore diameter is 400 nm. It is pretreated by an oxidation in flowing O_2 (10% in Ar) for 1 h at 400°C, a reduction by hydrogen (10% in Ar) for 2 h at 400°C and a subsequent conditioning for 12 h at 450°C using a feed of 2% NO and 1% CO in 100 ml/min (NTP[3]) flowing Ar.

The used fixed-bed reactor with external recycle loop is a special construction consisting of two concentric tubes of quartz glass. The reaction mixture flows upwards in the outer tube where it heats up preliminary and then downwards in the inner tube passing the catalytic bed, the catalyst is held in place by quartz wool. The reactor is described in detail in [9] and [13]. The reactor effluent is measured by a gas chromatograph for H_2, N_2O and CO_2 (Shimadzu GC-14A), an infrared detector for CO_2 (Ultramat 22P, Siemens) and a chemiluminescence analyser for NO_x (Thermo Environmental Instruments/10AR), described in [9] and [13]. Heat and mass transfer limitations are estimated by the Mears criteria and the Weisz-modul [13]. For the highest observed reaction rate the overheating of the catalyst particles is below 1°C and the effectiveness factor η is 0.98, thus external heat or internal mass limitations can be excluded.

In all experiments (except in the experiment shown in Figs. 2 and 3) the *outlet* mole fraction of NO_x in the reactor is held at a defined value. The inlet mole fractions of H_2 or O_2 are varied while maintaining the overall volume flow constant at 150 ml/min. Thus the recycle ratio φ ($\varphi=Q_{V,loop}/Q_{V,out}$) is always 138 corresponding to a space velocity of 6500 h^{-1}. Each experimental point is kept constant for 3.5 h.

Under the used conditions the recycle reactor is shown to hydrodynamically behave like an ideal

[3]NTP=normal conditions: 273 K, 1.013×10^5 Pa

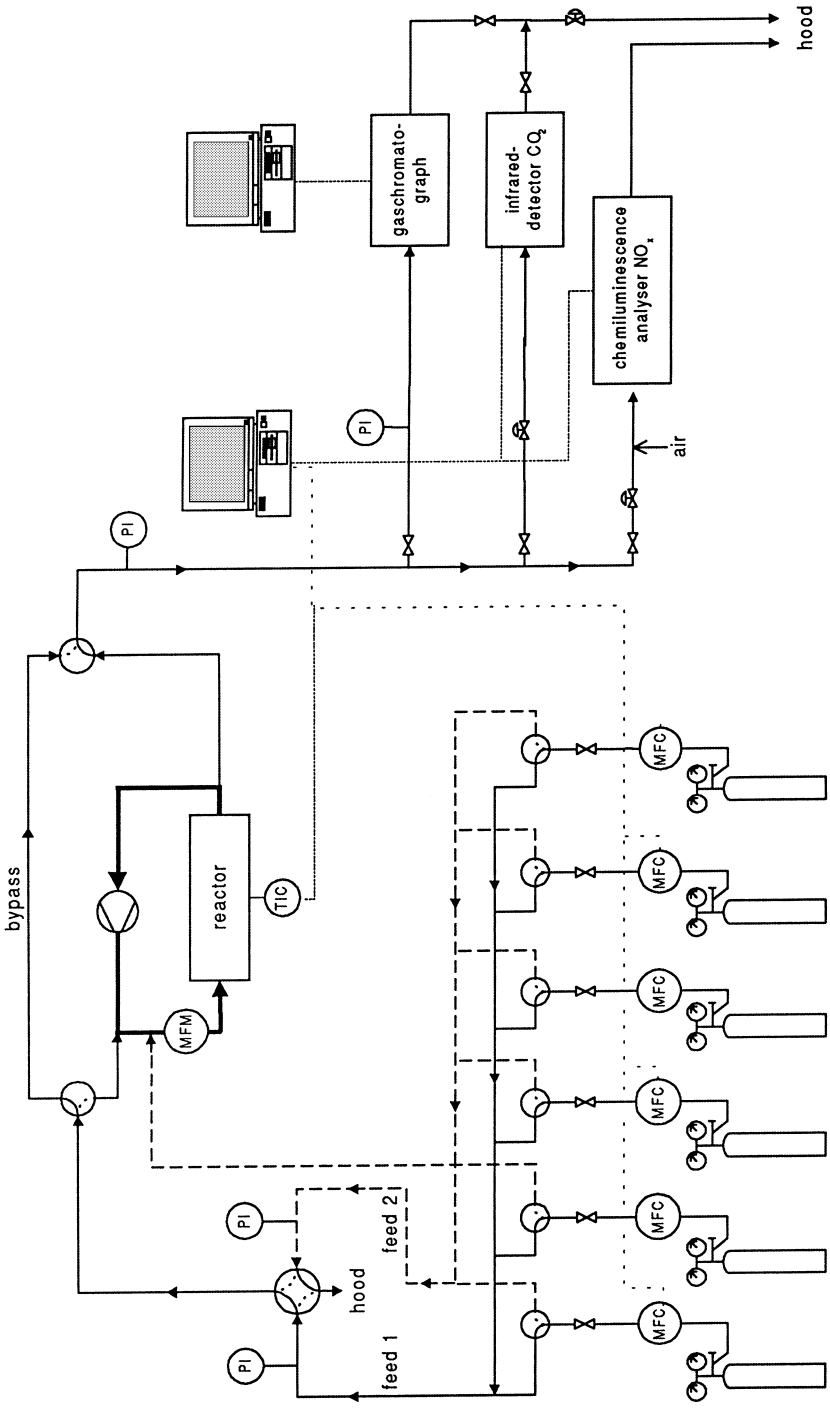

Fig. 1. Experimental set-up.

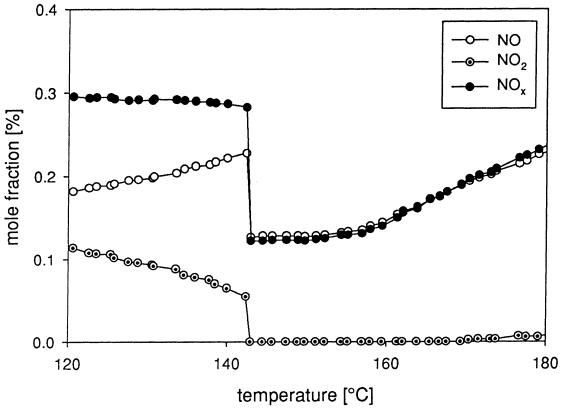

Fig. 2. Mole fractions during a temperature ramp of the $NO/H_2/O_2$ reaction on the Pt–Mo–Co catalyst (inlet conditions: 0.3% NO, 0.8% H_2, 8% O_2).

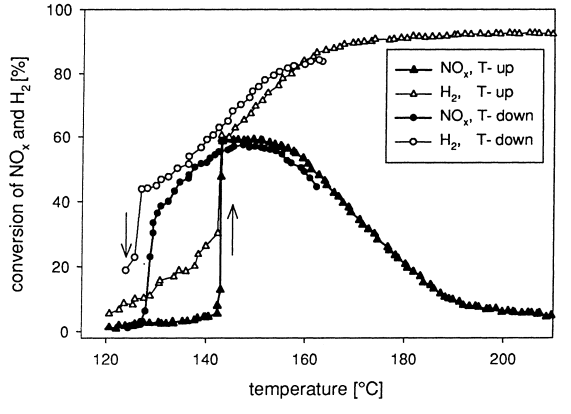

Fig. 3. Hysteresis of the $NO/H_2/O_2$ reaction during an increasing and decreasing temperature ramp (1.5°C/h) on a Pt–Mo–Co catalyst (inlet conditions: 0.3% NO, 0.8% H_2, 8% O_2, p=160 kPa).

continuous stirred tank reactor (CSTR) with a mean residence time of 192 s and a total reactor volume of 480 ml [13].

As the used mole fractions of reactants are small, the maximum possible difference of the overall volume flow Q_V is −2% at 100% conversion of NO and H_2. Changes of the volume flow rate Q_V as well as of the density can, therefore, be neglected. Conversion X, selectivity S and the yield Y can then be calculated as

$$X_i = \frac{y_{i,0} - y_i}{y_{i,0}} \quad i = \mathrm{NO} \text{ or } \mathrm{H_2} \quad (Q_V = \text{const.}) \qquad (1)$$

$$S_i = \frac{y_i}{y_{NO,0} - y_{NO}} \cdot \frac{|\nu_{NO}|}{|\nu_i|} \quad i = \mathrm{N_2}, \mathrm{N_2O} \quad (Q_V = \text{const.}) \qquad (2)$$

$$Y_i = \frac{y_i}{y_{H_2,0}} \cdot \frac{|\nu_{H_2}|}{|\nu_i|} \quad i = \mathrm{N_2}, \mathrm{N_2O} \text{ or } \mathrm{H_2O^*} \quad (Q_V = \text{const.}) \qquad (3)$$

The stoichiometric ratio λ is given by

$$\lambda = \frac{y_{NO,0} + 2y_{O_2,0}}{y_{H_2,0}} \qquad (4)$$

The reaction rate R_i of each species i is obtained by

$$R_i = \frac{(y_{i,0} - y_i)}{m_{cat}} \cdot \left(\frac{p \cdot Q_V}{RT}\right)_{NTP} \quad (Q_V = \text{const.}) \qquad (5)$$

The following reactions take place in the $NO/H_2/O_2$ system:

$$2\,NO + 2\,H_2 \rightarrow N_2 + 2\,H_2O \quad \text{reaction 1} \qquad (6)$$

$$2\,NO + H_2 \rightarrow N_2O + H_2O \quad \text{reaction 2} \qquad (7)$$

$$0.5\,O_2 + H_2 \rightarrow H_2O^* \quad \text{reaction 3} \qquad (8)$$

Furthermore the homogeneous oxidation of NO to NO_2 occurs (up to 30%), but is not considered separately. It is assumed that NO and NO_2 have a comparable reactivity: In Fig. 2 the mole fractions of NO_x ($NO+NO_2$), NO_2 and NO are plotted as a function of temperature. At 140°C about 20% of NO_x is present as NO_2 and at T>142°C (ignited state) no NO_2 is observed any more. It must be concluded that all NO_2 which was present at 140°C has reacted. Nevertheless, not only 100% NO_2 but also 50% of the present NO is consumed at 142°C. This indicates that the reactivity of the two species is of the same order of magnitude justifying that the two species are considered as a common NO_x species during the kinetic measurements [13]. The consecutive reaction of N_2O with H_2 was independently studied and shown to be negligible. The formation rate of water produced by reaction 3 (Eq. (8)) is determined by the mass balance and is always denoted by an asterix (H_2O^*).

$$R_{H_2O^*} = R_{H_2} - 2\,R_{N_2} - R_{N_2O} \qquad (9)$$

Furthermore, the formation rate of N_2 is calculated by

$$R_{N_2} = 0.5 \cdot R_{NO_x} - R_{N_2O} \qquad (10)$$

3. Results

3.1. Selectivity and N_2 yield

Since nitrous oxide is found to be an effective greenhouse gas, increasing attention is given in only producing N_2 and avoiding the formation of N_2O. The selectivity towards N_2 (S_{N_2}) is found to have the following tendencies (Table 1): increase with the higher partial pressures of O_2 and temperature and decrease with higher partial pressures of NO. However, the highest yield of N_2 is obtained for low partial pressures of O_2, high partial pressures of NO and H_2 and low temperatures. These conditions are not favourable for the N_2 selectivity compared to that toward N_2O. Higher partial pressures of O_2 and higher temperatures are advantageous for the N_2 selectivity, but this is counteracted by the disadvantage of increasing yields of water. Water is produced by reaction 1–3 (Eqs. (6)–(8)). The H_2O^* yield is found to have the following tendencies (Table 1): increase with increasing partial pressures of O_2 and temperature and decrease with increasing partial pressures of NO and H_2 (Table 1 and Fig. 4).

The selectivity of the reaction of hydrogen with nitric oxide in comparison with the reaction of hydrogen with oxygen is of interest in view of the efficiency of the catalyst. The ratio of the H_2 consumption of reaction 1 and 2 (Eqs. (6) and (7)) to the H_2 consumption by reaction 3 (Eq. (8)) is given by

$$S'_{1+2,3} = \frac{R_{H_2,1} + R_{H_2,2}}{2 \cdot R_{H_2,3}} \tag{11}$$

This corresponds to the ratio of the rate at which hydrogen reacts with nitric oxide to that at which it reacts with oxygen. Since there is a large excess of oxygen over NO (50–100-fold), most of the hydrogen

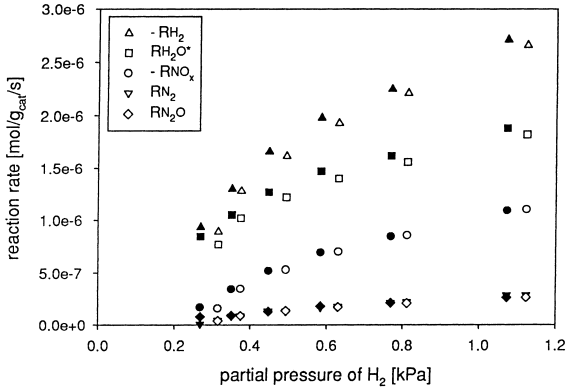

Fig. 4. Reaction rates of the $NO/H_2/O_2$ reaction (filled symbols) and reproduced run (open symbols) on a Pt–Mo–Co catalyst (0.32 kPa NO_x, 12.3 kPa O_2, T=142°C).

reacts with oxygen (50–95% of H_2). Therefore, $S'_{1+2,3}$ must be related to the ratio of nitrogen monoxide to oxygen f_{NO} (Eq. (12)).

$$S_{f_{NO}} = S'_{1+2,3}/f_{NO} = \frac{R_{H_2,1} + R_{H_2,2}}{2 \cdot R_{H_2,3}} \Big/ \frac{p_{NO}}{2 \cdot p_{O_2}} \tag{12}$$

A $S_{f_{NO}}$ value of one represents the case where hydrogen reacts with the two oxidants in the proportion of their presence in the gas phase. Higher values of $S_{f_{NO}}$ indicate that hydrogen reacts preferentially with nitrogen monoxide and lower values that hydrogen reacts preferentially with oxygen. The average value of $S_{f_{NO}}$ in the kinetic measurements is 3 for 142°C and decreases to 2 at 160°C. This signifies that the reaction rate of hydrogen with nitric oxide is in an average two to three times faster as compared to proportion of nitric oxide in the gas phase and that the reaction becomes less selective at higher temperatures.

Table 1
Average yields for N_2, N_2O and H_2O^* for different H_2 partial pressures

	142°C			160°C		
NO_x	0.16 kPa	0.32 kPa	0.16 kPa	0.16 kPa	0.32 kPa	0.16 kPa
O_2	7.3 kPa	7.3 kPa	16.6 kPa	7.3 kPa	7.3 kPa	16.6 kPa
$Y_{H_2O^*}$ (%)	58.7	47.9	69.8	82.7	69.4	89.3
Y_{N_2} (%)	14.9	17.1	8.8	9.4	17.4	4.0
Y_{N_2O} (%)	6.5	8.7	3.5	3.3	5.1	1.3
S_{N_2} (%)	53.7	49.6	55.4	59.0	63.0	61.2

3.2. Kinetics of the $NO/H_2/O_2$ reaction

An increasing as well as a decreasing temperature ramp, depicted in Fig. 3, show that below 127°C and above 142°C the NO_x conversion is the same within the experimental accuracy. In the temperature range from 127°C to 142°C a bistable behaviour is found. Coming from low temperatures the conversion of NO_x rests below 10% up to 142°C. At this temperature the reaction ignites and within some degrees the NO_x conversion increases to 60%. Up to 155°C it remains at 60% and for further increasing temperatures the conversion slowly decreases. For decreasing temperatures the conversion rests high for $T<142$°C and the reaction extincts only at 127°C. This shows that an autocatalytic behaviour is present for the $NO/H_2/O_2$ reaction. The observed hysteresis corresponds to a saddle-node bifurcation [13]. In a saddle-node bifurcation a system jumps from one activity branch to another activity branch after a small perturbation without the occurrence of oscillations.

For temperatures above 140°C a model to describe the reaction kinetics can be established. Fig. 4 summarises the formation or consumption rates of N_2O, N_2, H_2O^*, NO_x and H_2 for different partial pressures of H_2 at 142°C. The reproducibility of the experiments is manifested by a repeated run given by the open symbols. All of the reaction rates increase with increasing partial pressures of H_2. A comparison between the consumption rates of H_2 and the formation rate of H_2O^* shows again that the majority of the consumed hydrogen reacts with oxygen. It was observed that below a H_2 partial pressure of 0.28 kPa ($y_{H_2,0} = 0.8\%$) the reaction rate decreased sharply and the rate was then within the experimental error. Thus, for the onset of the reaction p_{H_2} has to be larger than a certain minimum value.

Exemplary experimental results for the formation of N_2, N_2O and H_2O^* are shown in Figs. 5–7, superimposed by calculated curves of the proposed model (Eqs. (13)–(15)). Figs. 5 and 6 resume the results at different partial pressures of NO and O_2, respectively. The higher the partial pressure of NO or O_2 the more the onset of the reaction is shifted toward higher partial pressures of hydrogen. The higher the temperature the more the onset of the reaction is shifted to low partial pressures of H_2 pressures as demonstrated in Fig. 7. The 'shift' is an important feature of the kinetic behaviour of the reaction and is taken into account in the model.

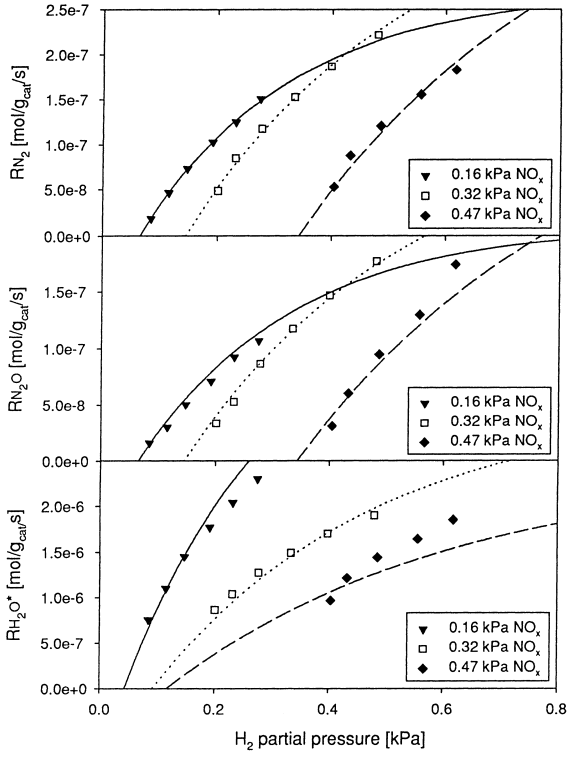

Fig. 5. Measured formation rates of N_2, N_2O and H_2O^* for different partial pressures of NO and calculated curves by Eqs. (13)–(15) for the $NO/H_2/O_2$ reaction (12.1 kPa O_2, T=149°C).

Based on the experimental results a developed model describes three parallel reactions: formation of N_2 by Eq. (6), of N_2O by Eq. (7) and of H_2O^* by Eq. (8). The reactions are supposed to be irreversible and all of the products to desorb fast, which is the case on Pt [14,15]. The reaction rates assuming a Langmuir–Hinshelwood mechanism between competing adsorbed NO, O_2 and H_2 can be written as:

- formation rate of N_2:

$$R_{N_2} = k_{N_2} \cdot \frac{K_{NO} p_{NO} \cdot K_{H_2}(p_{H_2} - p_0)}{(1 + K_{NO} p_{NO} + K_{H_2}(p_{H_2} - p_0) + K_{O_2} p_{O_2})^2} \quad (13)$$

- formation rate of N_2O:

$$R_{N_2O} = k_{N_2O} \cdot \frac{K_{NO} p_{NO} \cdot K_{H_2}(p_{H_2} - p_0)}{(1 + K_{NO} p_{NO} + K_{H_2}(p_{H_2} - p_0) + K_{O_2} p_{O_2})^2} \quad (14)$$

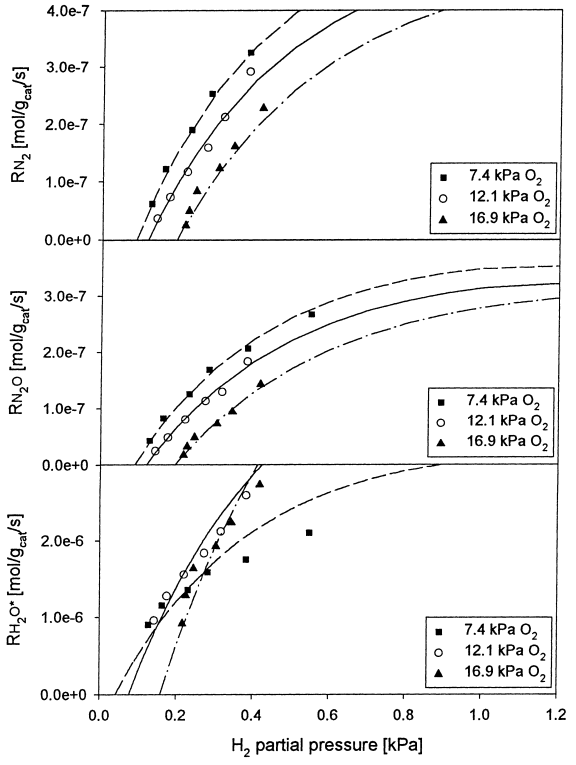

Fig. 6. Measured formation rates of N_2, N_2O and H_2O^* for different partial pressures of O_2 and calculated curves by Eqs. (13)–(15) for the NO/H_2/O_2 reaction (3.2 kPa NO_x, T=156°C).

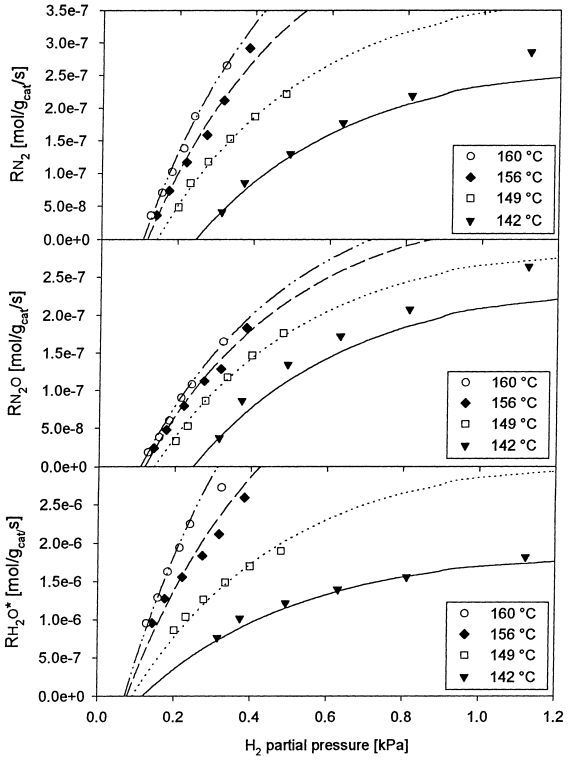

Fig. 7. Measured formation rates of N_2, N_2O and H_2O^* at different temperatures and calculated curves by Eqs. (13)–(15) for the NO/H_2/O_2 reaction (0.32 kPa NO_x, 12.1 kPa O_2).

- formation rate of H_2O^*:

$$R_{H_2O^*} = k_{H_2O^*} \cdot \frac{K_{O_2} p_{O_2} \cdot K_{H_2}(p_{H_2} - p_0')}{(1 + K_{NO} p_{NO} + K_{H_2}(p_{H_2} - p_0') + K_{O_2} p_{O_2})^2} \quad (15)$$

The model considers the adsorption of NO, H_2 and O_2 expressed by three adsorption equilibrium constants K_{NO}, K_{H_2} and K_{O_2} ($K_i = k_{i,ad}/k_{i,des}$). Identical adsorption equilibrium constants of NO, H_2 and O_2 are used in the three expressions, since the reactions take place at the same surface with the same adsorption and desorption rates for each species. The parameters p_0 and p_0' are introduced to account for the 'shift' of the curves demonstrated in Figs. 5 and 6.

The model with the three formation rates Eqs. (13)–(15) is introduced in the commercially available program *SimuSolv*® and subsequently the six parameters k_{N_2}, k_{N_2O}, $k_{H_2O^*}$, K_{NO}, K_{H_2} and K_{O_2} are optimised at the same time for a constant temperature using a Nelder–Mead search. The parameters p_0 and p_0' are estimated graphically and adjusted for each experiment in order to give the best fit. The dependence of p_0 can be reasonably expressed by an empirical relationship (Eq. (16)).

$$p_0 = (-a \cdot T + b) \cdot \exp(c \cdot p_{NO} + d \cdot p_{O_2}) \quad (16)$$

a=4.95×10^{-4} kPa K^{-1}, b=0.224 kPa, c=4.59 kPa^{-1} and d=8.25×10^{-2} kPa^{-1}

This relationship characterises the increase of p_0 with increasing partial pressures of NO and O_2 as well as the decrease with increasing temperatures. p_0' is roughly about 0.5·p_0, but exhibits large variations, thus it hasn't been fitted.

The determined reaction rate constants k_n and the equilibrium rate constants of adsorption K_i follow the Arrhenius law (Eq. (17)) and the van't Hoff law

Table 2
Activation energies or heat of adsorption and preexponential factors of the model Eqs. (13)–(15) for the $NO/H_2/O_2$ reaction

	$E_{a,n}$ (kJ/mol)	k_{n0} (mol/g/s)		ΔH_i (kJ/mol)	K_{i0} (kPa^{-1})
k_{N_2}	76.9 (±4.6)	8157	K_{H_2}	−58.6 (±5.0)	2.12E−07
k_{N_2O}	45.0 (±8.9)	0.716	K_{NO}	−77.2 (±3.5)	2.83E−09
$k_{H_2O^*}$	129.0 (±5.6)	4.92E+11	K_{O_2}	−96.5 (±2.8)	1.19E−13
k_{NO}[a]	63.16 (±6.5)	585			

[a]Calculated by Eq. (10).

(Eq. (18)), respectively.

$$k_n = k_{n0} \cdot \exp(-E_{a,n}/RT) \quad (17)$$

$$K_i = k_{\mathrm{ad},i}/k_{\mathrm{des},i} = k_{\mathrm{ad},i0}/k_{\mathrm{des},i0} \cdot \exp(-(E_{\mathrm{ad},i} - E_{\mathrm{des},i})/RT) = K_{i0} \cdot \exp(-\Delta H_i/RT) \quad (18)$$

From Arrhenius plots activation energies and preexponential factors are estimated by the slope and the intersect with the ordinate, respectively, resumed in Table 2. Determined regression factors of the straight lines vary from 0.927 to 0.998. The agreement between the experimental and the calculated reaction rates is good, the relative error is within 15% (Fig. 8).

3.3. Enhancement of the NO reduction by O_2

With competing Langmuir–Hinshelwood expressions for the NO removal and the H_2O^* formation one expects an increase of the formation rate of H_2O^* and a decrease of the consumption rate of NO_x with higher partial pressures of O_2.

In Fig. 9 the reaction rates of NO_x and H_2O^* are plotted versus the inlet mole fraction of O_2 and the stoichiometric ratio λ at different temperatures. One can note that the reaction rate of NO_x increases by a factor of 3 upon introduction of 2% O_2 (λ=4) compared to the reaction rate for 0.52% O_2 (λ=1). For higher mole fractions of O_2 the reaction rate decreases, thus the reaction rate of NO_x passes through a maximum at a stoichiometric ratio of λ=4. In parallel to the increase of the NO_x reaction rate at low inlet mole fractions of O_2 a strong decrease in the H_2O^* formation takes place. For higher temperatures, the maximum value of the NO_x reaction rate increases and the maximum is slightly shifted toward lower inlet mole fractions of O_2 (Fig. 9). Such an enhancement of the NO reduction for low pressures of oxygen cannot be explained by the proposed Langmuir–Hinshelwood mechanism. Fig. 10 presents the results upon an increasing and decreasing variation of O_2. The two

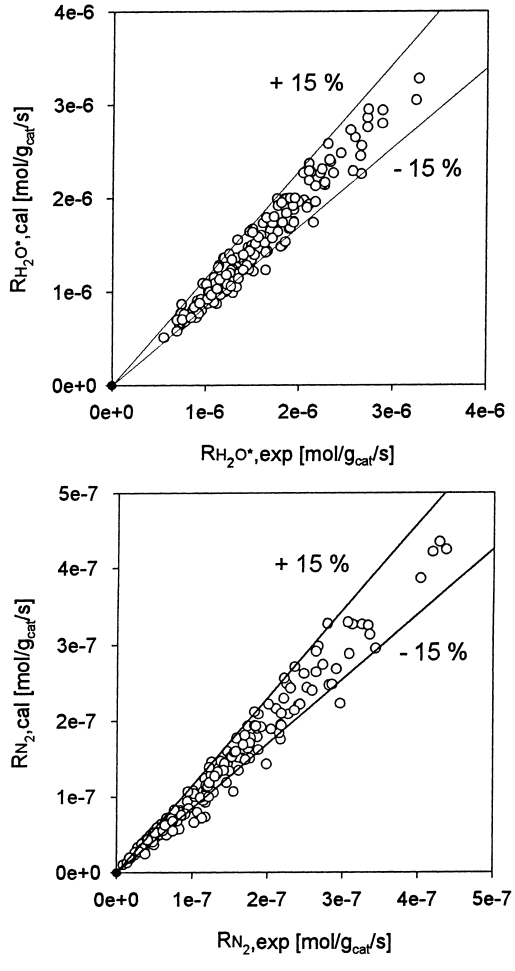

Fig. 8. Formation rates of N_2 and H_2O^* of the $NO/H_2/O_2$ reaction: experimental measurements versus calculated values by Eqs. (13)–(15).

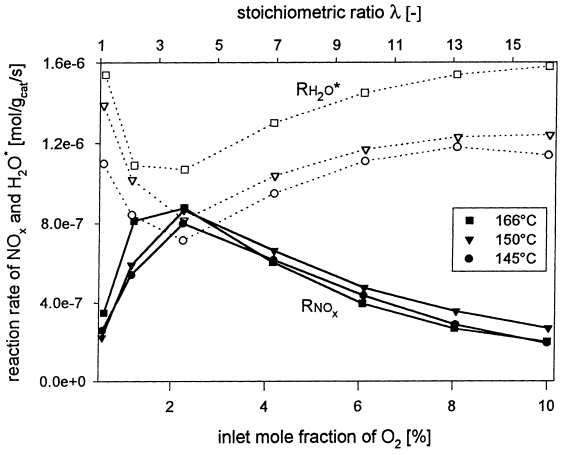

Fig. 9. Reaction rates of NO_x and H_2O^* as function of the inlet mole fraction of O_2 and corresponding stoichiometric ratio λ at different temperatures (1.25% H_2 (inlet), 0.2% NO_x, p=167 kPa).

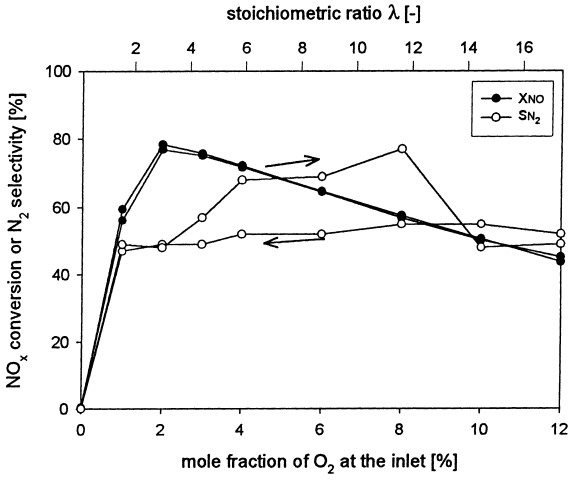

Fig. 10. NO_x conversion and N_2 selectivity versus the inlet mole fraction of O_2 and corresponding stoichiometric ratio λ for increasing and decreasing mole fractions of O_2 (1.4% H_2 (inlet), 0.2% NO_x, T=156°C, p=159 kPa).

curves superimpose perfectly and no hysteresis arises. The selectivity toward N_2 is higher during the increase of O_2, thus coming from reducing conditions. This might be rationalised in an increase of the NO dissociation on reduced Pt sites as proposed by [16].

In this context another interesting feature is observed. In Fig. 11 the reaction rate of NO_x for different inlet partial pressures of O_2 is plotted versus

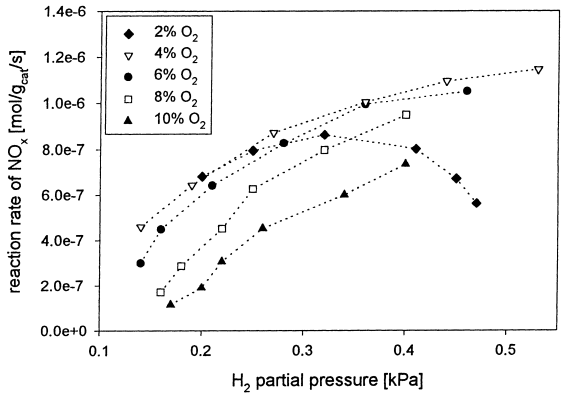

Fig. 11. Reaction rate of NO_x as function of the H_2 partial pressure for different inlet mole fractions of O_2 (0.2% NO_x, T=157°C, p=164 kPa).

the partial pressure of H_2. Here the reaction rate of NO_x as well as of H_2O^* (not shown) increase with higher partial pressures of H_2 as was already found during the kinetic measurements. However, for 2% O_2 the reaction rate of NO_x passes through a maximum and decreases with higher partial pressures of H_2. At the same time the reaction rate of H_2O^* increases strongly (not shown). Thus, the positive reaction order of hydrogen changes into a negative reaction order of H_2. A negative reaction order of H_2 can also not be explained by a Langmuir–Hinshelwood mechanism.

4. Discussion

4.1. Kinetics of the $NO/H_2/O_2$ reaction

The kinetic study is carried out at sufficiently high temperatures (142–160°C) where the bistable behaviour is overcome and λ>4 (with partial pressures of O_2 above 4%). In this region the reaction rate of NO_x decreases with increasing partial pressures of O_2 due to the increase of the competing H_2/O_2 reaction. The partial pressure of H_2 has to be larger than a certain minimum value p_0, for lower partial pressures of H_2 no reaction takes place. Both of these features are well described by the proposed modified Langmuir–Hinshelwood expressions.

The results of the kinetic study reveal that NO is the most strongly adsorbed species whereas O_2 is only weakly adsorbed. The order $E_{a,H_2O^*} > E_{a,N_2} > E_{a,N_2O}$

(129 kJ/mol>76.9 kJ/mol>45 kJ/mol) is in agreement with the experimental findings that the selectivity of H_2O^* as well as the ratio S_{N_2}/S_{N_2O} increase with increasing temperature. The same tendency is found by Wildermann on a Pt–Mo catalyst [8], who determined a similar activation energy for the N_2O formation (46 kJ/mol) but slightly smaller activation energies for the formation of N_2 (57 kJ/mol) and the O_2/H_2 reaction (93 kJ/mol). The determined activation energy of the NO_x consumption via Eq. (10) is in good correspondence with the value of 62.8 kJ/mol given by Otto and Yao for the reduction of NO by H_2 over Pt/γ-Al_2O_3 in an excess of NO [17]. The value of the heat of adsorption of H_2 is in good agreement with other reported values on platinum: 46 kJ/mol [18], 68.1 kJ/mol [19] and 51.8 kJ/mol [20]. Values of desorption energies of O_2 found in the literature (230 kJ/mol [21]) are substantially higher than the heat of adsorption found in this study. This discrepancy might be due to the fact that the dissociative adsorption of oxygen is an activated process. In this case the heat of adsorption is lower than the activation energy for desorption. Only when the adsorption is non-activated (E_{ad}=0) the heat of adsorption can be directly compared to the desorption energy [22].

The mechanism of the reaction can be represented by the following elementary steps.

$$NO + Z \leftrightarrow NO_{ad} \quad (19)$$

$$H_2 + 2\,Z \leftrightarrow 2\,H_{ad} \quad (20)$$

$$O_2 + 2\,Z \leftrightarrow 2\,O_{ad} \quad (21)$$

$$NO_{ad} + Z \rightarrow N_{ad} + O_{ad} \quad (22)$$

$$2\,N_{ad} \rightarrow N_2 \uparrow + 2\,Z \quad (23)$$

$$NO_{ad} + N_{ad} \rightarrow N_2O \uparrow + 2\,Z \quad (24)$$

$$O_{ad} + H_{ad} \rightarrow OH_{ad} + Z \quad (25)$$

$$OH_{ad} + H_{ad} \rightarrow H_2O \uparrow + 2\,Z \quad (26)$$

In this mechanism Z represents a free adsorption site and X_{ad} an adsorbed species X. The adsorption of H_2 and O_2 on platinum is reported to be dissociative [14,17,23]. The products N_2, N_2O and H_2O are assumed to desorb easily on platinum ([14], p. 544).

In the region where the Langmuir–Hinshelwood model describes the kinetics of the reaction the adsorption of all species as well as the dissociation of NO easily take place and the surface reactions Eqs. (23) and (26) are the rate-determining steps. In this case the product distribution corresponds to the well-established competition between NO_{ad}, N_{ad} and H_{ad} [16]. For conditions where more N_{ad} is present, that are high temperatures and low partial pressures of NO, the selectivity towards N_2 increases.

In this study it is furthermore found that a minimum partial pressure of H_2 (p_0 in the Langmuir–Hinshelwood model) is necessary to start the reaction. This minimum partial pressure of H_2 is smaller at higher temperatures. It is well-accepted that the onset of the NO/H_2 reaction is linked to the beginning of the NO dissociation [24]. Obviously the NO dissociation depends not only on temperature, but also on the partial pressure of H_2. Since increasing quantities of hydrogen shift the onset of the reaction toward lower temperatures the observed behaviour can be interpreted as an enhancement of the NO dissociation by hydrogen.

Several authors report from an enhancement of reaction rates by hydrogen, e.g. for the CO/O_2 reaction on Pt [25–27] and for the NO/CO reaction on Pt [28,29]. The exact mechanism is unclear for both reactions. Furthermore, it was reported that the NO dissociation is promoted by H_{ad} on platinum [23,24,30–32]. During co-adsorption of NO and CO at 160°C on a Au/NaY catalyst Salama et al. did not observe a -NCO band [30]. Only upon introduction of H_2 an intense -NCO developed, indicating the presence of N_{ad}. The authors conclude that the H-atom had promoted the N–O bond fission. Hecker and Bell found a positive order dependence of the NO/H_2 reaction on H_2, although they assume that the NO dissociation is the rate-limiting step [32]. The authors postulate that the NO dissociation proceeds with the assistance of an adsorbed H atom via the following mechanism:

$$NO_{ad} + H_{ad} \rightarrow N_{ad} + OH_{ad} \quad (27)$$

However, such a mechanism is not consistent with the observed behaviour in the present study, because it would lead to a slow increase of the NO removal with temperature and not to an autocatalytic onset as in Fig. 3. Another mechanism is proposed by Pirug and Bonzel on Pt [24]. By flash desorption experiments they found that the activation energy for NO dissociation decreases with decreasing coverages of NO. They suggest that co-adsorbed hydrogen can displace

molecularly adsorbed NO leading to the needed decrease in NO coverage where the NO dissociation can take place. This mechanism is coherent with the observed features in the present study: thus, the autocatalytic onset of the reaction is not solely attained by higher temperatures but also through a displacement of surface NO by adsorbed hydrogen. At higher H_2/NO ratios the competitive adsorption of H_2 and NO is more and more shifted toward hydrogen. As a consequence the onset of the reaction is shifted to lower temperatures. This is in perfect agreement with the observed decrease of the minimum partial pressure of hydrogen p_0 at higher temperatures. The mechanism is also coherent with an increase in p_0 for higher partial pressures of NO. Obviously more hydrogen is needed to decrease the NO coverage sufficiently. The increase of p_0 with higher quantities of oxygen is also in agreement with this model. To decrease the NO coverage sufficiently the supplementary removal of O_{ad} increases the H_2 consumption and thus p_0.

As hydrogen has a lower adsorption energy on platinum as NO_{ad} the question arises if adsorbed hydrogen atoms are actually capable to displace NO_{ad}. Confirmation is given by some groups who found that atomic hydrogen is able to displace small amounts of molecularly adsorbed NO on Pt(111) surfaces presaturated with NO [15,33]. Nonetheless, the proposed mechanism is based on the hypothesis that although H_{ad} can displace NO_{ad}, H_{ad} does not further inhibit the dissociation. This seems possible as hydrogen is quite small and thus very flexible and may even spill-over to the support.

4.2. Enhancement of the NO reduction by O_2

In three-component reactions NO/O_2/CO or NO/O_2/H_2 the reducing agent is partitioned between NO and O_2. If NO and O_2 compete for the same surface sites, as assumed in the proposed Langmuir–Hinshelwood model, the rate of NO reduction should always decrease in the presence of oxygen. However, for O_2 partial pressures below 2% the reaction rate of NO_x increases strongly with increasing partial pressures of O_2, while the H_2O^* formation decreases (Fig. 9). This increase is not autocatalytic and no bistable behaviour arises during increasing and decreasing variation of O_2 (Fig. 10). In this context it is also interesting to note that for small O_2 and high H_2 partial pressures the reaction order of hydrogen becomes negative (Fig. 11).

It is known that the mutual influence of reactants in heterogeneous catalytic reactions can lead to an enhancement of reaction rates under certain conditions [34]. Thus, several authors reported of a promoting effect of oxygen on the NO/CO reaction on Pt catalysts when stoichiometric or reducing conditions were previously used [35–37]. One of the first were Alikina et al. who found increasing NO conversions on a Pt/γ-Al_2O_3 catalyst up to λ=1.15 [35]. As they used a ratio CO : NO of 1.63 they supposed that with increasing O_2 concentrations platinum passes in a partially oxidised state lowering the Pt–CO bond. Barton reported that the addition of small amounts of oxygen up to λ=1.6 resulted in a significant increase in the NO conversion on a $LaMnPtO_3$ catalyst at 250°C (ratio CO : NO=1) [37]. The influence of oxygen on the NO/NH_3 reaction on Pt(100) was also reported to be accelerating [38]. For both reactions the exact mechanism is still subjected to speculations and the enhancing role of oxygen is not yet fully understood.

More commonly known is the promoting effect of oxygen of the NO reduction by hydrocarbons [39,40]. This has recently been reported for Pt-containing catalysts with oxygen contents up to 2% [4,16,31]. However, also here the mechanism is still unclear. The promoting effect of oxygen is attributed to either a partial oxidation of the hydrocarbon or the higher activity of the formed NO_2 [40]. Other authors explain it in terms of an oxidative removal of blocking carbonaceous species on the active platinum sites [16]. For the NO/H_2 reaction a promoting effect of oxygen has not been reported up to now for a platinum containing catalyst. Jones et al. [7] and Heil [41] notified a reduced NO removal upon an increase of the oxygen level.

In the present study a mechanism as the removal of a carbonaceous species or an activation of the hydrocarbon cannot account to the enhancement by O_2. A higher activity of NO_2 or of nitrates formed on the surface of the catalyst might be considered. Nonetheless, this does not explain why in a large excess of hydrogen the order of H_2 is negative.

Based on the results found in the present study the following mechanism is, therefore, proposed: abundant surface hydrogen separates the N atoms formed

by dissociation decreasing the likelihood that two N atoms are in close proximity and thus the N-pairing. In this case the reaction order of hydrogen becomes negative, although hydrogen enhances the NO dissociation. The enhancement by oxygen is then due to the removal of the abundant H_{ad}. When the recombination of N_{ad} is again possible, O_2 exercises the expected negative order influence on the NO reduction. The reason that no NH_3 is formed might be due to the fact that the promoting effect of oxygen is measured in oxidising atmospheres for stoichiometric ratios up to λ=4. This is among the highest ratios reported for such an enhancement. The slight shift of the maximum of NO_x conversion at higher temperatures towards lower mole fractions of O_2 in Fig. 9 can be rationalised in a higher mobility of the surface species and, therefore, less inhibition by H_{ad}. This mechanism does not include a change in the reaction mechanism nor of the catalyst surface structure and is fully supported by the absence of a hysteresis upon variation of the oxygen content as shown in Fig. 10.

5. Conclusions

The proposed mechanism based on a coverage-dependant activation energy of NO dissociation elucidates all of the here observed reaction features. Low temperatures lead to high NO coverages impeding the NO dissociation. When the surface coverage decreases with temperature the autocatalytic character leads to a sudden onset of the NO/H_2 reaction resulting in bistability and hysteresis. Hydrogen promotes the dissociation of NO by decreasing the NO coverage and thus the activation energy for dissociation down to a value, where the dissociation can occur. However, high coverages of H_{ad} reduce the likelihood of two N_{ad} to recombine and the reaction rate of NO_x decreases. In this study an accelerating effect of oxygen on the NO/H_2 reaction on Pt is for the first time reported (up to λ=4). It is attributed to the lowering of abundant H_{ad} by O_2 permitting again the N-pairing.

6. Notation

c_i	mol/m^3	concentration of species i
E_a, E_{ad}, E_{des}	kJ/mol	activation energy of reaction, adsorption, desorption
ΔH_i	kJ/mol	adsorption enthalpy of species i
K_i	1/Pa	equilibrium constant of adsorption of species i
k_n		reaction rate constant of reaction n
m_{cat}	g	mass of catalyst
p_i	Pa	partial pressure of species i
R	J/mol/K	ideal gas law constant
R_i	mol/g/s	reaction rate of species i
S_i	–	selectivity of species i
Q_V	m^3/s	volume flow rate
X_i	–	conversion of species i
$y_{i,0}$	–	inlet mole fraction of species i
y_i	–	mole fraction of species i
Y_i	–	yield of species i
λ	–	stoichiometric ratio
ν_i	–	stoichiometric coefficient of species i

Acknowledgements

Financial support by the Swiss National Science Foundation is gratefully acknowledged.

References

[1] S.E. Voltz, C.R. Morgan, D. Liederman, S.M. Jacob, Ind. Eng. Chem. Prod. Res. Dev. 12 (1973) 294.
[2] R. Burch, P.J. Millington, Catal. Today 26 (1995) 185.
[3] R. Burch, P.J. Millington, Catal. Today 29 (1996) 37.
[4] G. Zhang, T. Yamaguchi, H. Kawakami, T. Suzuki, Appl. Catal. B 1 (1992) L15.
[5] A. Obuchi, A. Ohi, M. Nakamura, A. Ogata, K. Mizuno, H. Ohuchi, Appl. Catal. B 2 (1993) 71.
[6] A. Lamb, E.L. Tollefson, Can. J. Chem. Eng. 53 (1975) 68.
[7] J.H. Jones, J.T. Kummer, K. Otto, M. Shelef, E.E. Weaver, Environ. Sci. Technol. 5 (1971) 790.
[8] A. Wildermann, Entwicklung eines Wasserstoff - SCR - Katalysators zu NO_x - Minderung in Rauch - bzw. Abgasen, Ph.D. work, University of Erlangen, Nürnberg, 1994.
[9] B. Frank, R. Lübke, G. Emig, A. Renken, Chem.-Ing.-Tech., accepted for publication (July 1998), English translation in Chem. Eng. Tech.
[10] T. Tanaka, K. Yokota, N. Isomura, H. Doi, M. Sugiura, Appl. Catal. B 16 (1998) 199.
[11] G.P. Ansell, P.S. Bennett, J.P. Cox, J.C. Frost, P.G. Gray, A.-M. Jones, R.R. Rajaram, A.P. Walker, M. Litorell, G. Smedler, Appl. Catal. B 10 (1996) 183.

[12] R. Mannila, T. Salmi, H. Haario, M. Luoma, M. Härkönen, J. Sohlo, Appl. Catal. B 7 (1996) 179.
[13] B. Frank, Reduction of NO by CO and H_2 on Pt–Mo supported catalysts – stationary and dynamic behaviour, Ph.D. work, Swiss Federal Institute of Technology, Lausanne, 1997.
[14] V. Ponec, C. Bond, Catalysis by Metals and Alloys, vol. 95, Elsevier, Amsterdam, 1995.
[15] J.L. Gland, E.B. Kollin, J. Catal. 68 (1981) 349.
[16] R. Burch, P.J. Millington, A.P. Walker, Appl. Catal. B 4 (1994) 65.
[17] K. Otto, H.C. Yao, J. Catal. 66 (1980) 229.
[18] P.R. Norton, P.J. Richards, Surf. Sci. 41 (1974) 293.
[19] M. Procop, J. Völter, Surf. Sci. 33 (1972) 69.
[20] G. Papapolymerou, A.G. Botis, A.D. Papargyris, X.D. Spiliotis, J. Mol. Catal. 84 (1993) 267.
[21] B.E. Nieuwenhuys, Surf. Sci. 126 (1983) 307.
[22] B.E. Nieuwenhuys, in: R.W. Joyer, R.A.V. Santen (Eds.), Elementary Reaction Steps in Heterogeneous Catalysis, Kluwer Academic Publishers, Dordrecht, 1993, 155 pp.
[23] M. Uchida, A.T. Bell, J. Catal. 60 (1979) 204.
[24] G. Pirug, H.P. Bonzel, J. Catal. 50 (1977) 64.
[25] D.W. Dabill, S.J. Gentry, H.B. Holland, A. Jones, J. Catal. 53 (1978) 164.
[26] H. Muraki, S. Matunaga, H. Shinjoh, M.S. Wainwright, D.L. Trimm, J. Chem. Technol. Biotechnol. 52 (1991) 415.
[27] S.H. Oh, R.M. Sinkevitch, J. Catal. 142 (1993) 254.
[28] S.J. Tauster, L.L. Murrell, J. Catal. 53 (1978) 260.
[29] R. Dümpelmann, N.W. Cant, D.L. Trimm, in: A. Frennet, J.-M. Bastin (Eds.), Catalysis and Automotive Pollution Control III, Studies in Surface Science and Catalysis, vol. 96, Elsevier, Amsterdam, 1995, 123 pp.
[30] T.M. Salama, R. Ohnishi, T. Shido, M. Ichikawa, J. Catal. 162 (1996) 169.
[31] R. Burch, T.C. Watling, Catal. Lett. 37 (1996) 51.
[32] W.C. Hecker, A.T. Bell, J. Catal. 92 (1985) 247.
[33] M.Y. Smirnov, V.V. Gorodetskii, A.R. Cholach, Bulgar. Acad. Sci. 22/3/4 (1989) 586.
[34] Y.I. Pyatnitsky, Appl. Catal. A 113 (1994) 9.
[35] G.M. Alikina, A.A. Davydov, I.S. Sazonova, V.V. Popovskii, Kinet. Katal. 27 (1986) 758.
[36] J. Regalbuto, D.J. Kaul, E.E. Wolf, Int. Congress Catal. (1984) 253.
[37] J. Barton, Collect. Czech. Chem. Commun. 55 (1990) 1935.
[38] M.F.H. Tol, J. Siera, P.D. Cobden, B.E. Nieuwenhuys, Surf. Sci. 274 (1992) 63.
[39] H. Hamada, Y. Kintaichi, M. Sasaki, T. Ito, Appl. Catal. 70 (1991) L15.
[40] M. Sasaki, H. Hamada, Y. Kintaichi, T. Ito, Catal. Lett. 15 (1992) 297.
[41] G. Heil, Untersuchung der heterogen katalysierten Reduktion von Stickoxiden mit Wasserstoff, Ph.D. work, University of Karlsruhe, 1995.